



HIGH-TEMPERATURE FRACTURE AND FATIGUE RESISTANCE OF A DUCTILE β -TiNb REINFORCED γ -TiAl INTERMETALLIC COMPOSITE

K. T. VENKATESWARA RAO¹ and R. O. RITCHIE^{2†}

¹Advanced Cardiovascular Systems, Guidant Corporation, Santa Clara, CA 95052-8167, and

²Department of Materials Science and Mineral Engineering, University of California, Berkeley, CA 94720, U.S.A.

(Received 12 August 1997; accepted 16 March 1998)

Abstract—The high-temperature fatigue-crack propagation and fracture resistance of a model γ -TiAl intermetallic composite reinforced with 20 vol.% ductile β -TiNb particles is examined at elevated temperatures of 650 and 800°C and compared with behavior at room temperature. TiNb reinforcements are found to enhance the fracture toughness of γ -TiAl, even at high temperatures, from about 12 to ~40 MPa m^{1/2}, although their effectiveness is lower compared to room temperature due to the reduction in strength of TiNb particles. Under monotonic loading, crack-growth response in the composite is characterized by resistance-curve behavior arising from crack trapping, renucleation and resultant crack bridging effects attributable to the presence of TiNb particles. In addition, crack-tip blunting associated with plasticity increases the crack-initiation (matrix) toughness of the composite, particularly at 800°C, above the ductile-to-brittle transition temperature (DBTT) for γ -TiAl. High-temperature fatigue-crack growth resistance, however, is marginally degraded by the addition of TiNb particles in the C–R (edge) orientation, similar to observations made at room temperature; premature fatigue failure of TiNb ligaments in the crack wake diminishes the role of bridging under cyclic loading. Both fatigue and fracture resistance of the composite are slightly lower at 650°C (just below the DBTT for TiAl) compared to the behavior at ambient and 800°C. Overall, the beneficial effect of adding ductile TiNb reinforcements to enhance the room-temperature fracture and fatigue resistance of γ -TiAl alloys is retained up to 800°C, in air environments. There is concern, however, regarding the long-term environmental stability of these composite microstructures in unprotected atmospheres. © 1998 Acta Metallurgica Inc. Published by Elsevier Science Ltd. All rights reserved.

1. INTRODUCTION

Titanium aluminide alloys based on the γ -TiAl intermetallic compound are currently under active development as high-temperature materials for integrated high-performance turbine engines and other structural applications in hypersonic and high-speed civil transport vehicles [1–7]. These efforts are in part aimed at improving their low room-temperature tensile ductility and fracture toughness, both factors which restrict the potential use of γ -TiAl despite its excellent high-temperature properties [3–11]. Alloying and composite reinforcement methods have been explored to toughen γ -TiAl with considerable success. In the former approach, small additions of Cr, V, Mo and Nb combined with novel thermo-mechanical treatments yield two-phase ($\gamma + \alpha_2$) microstructures with improved toughness, due to such mechanisms as crack deflection, uncracked (shear) ligament bridging and mechanical twinning [5–7]. In the latter approach, ductile TiNb, Nb or Ti–6Al–4V particles are incorporated in the microstructure to promote toughness by crack trapping and resulting crack bridging mechanisms [8–13].

Previous work [12,13] on model ductile-phase toughened γ -TiAl composites has shown that substantial improvements in fracture resistance can be achieved at room temperature. For example, by adding ~10 vol.% of TiNb particles to γ -TiAl, the crack-initiation toughness can be increased to ~16 MPa m^{1/2}, nearly twice that of pure γ -TiAl (~8 MPa m^{1/2}). Fracture resistance increases with further crack extension exhibiting resistance-curve (or R-curve) behavior primarily due to bridging by unbroken TiNb ligaments in the crack wake, with concurrent benefits from crack trapping by particles and renucleation effects. The degree of toughening under monotonic loading increases with volume fraction and strength of the reinforcement phase (stronger TiNb particles yield higher toughness compared to Nb), and is independent of particle orientation.

In contrast, particle orientation effects are significant under cyclic loading. Both TiNb and Nb reinforcements provide a modest increase in fatigue resistance of γ -TiAl, but *only* in the face (C–L) orientation where faces of pancake-shaped particles are oriented normal to the crack plane. Conversely, in the edge (C–R) orientation, where particle edges are oriented perpendicular to the crack plane, TiNb

†To whom all correspondence should be addressed.

particles actually *degrade* the fatigue-crack growth resistance of the composite relative to unreinforced γ -TiAl. This markedly reduced influence of ductile-phase toughening during cyclic crack growth in TiAl composites is primarily due to the premature

fatigue failure of ductile ligaments, which in turn restricts the development of a bridging zone in the crack wake. Interface properties are also critical; weakly bonded Nb particles offer better fatigue-crack growth resistance than TiNb particles that are

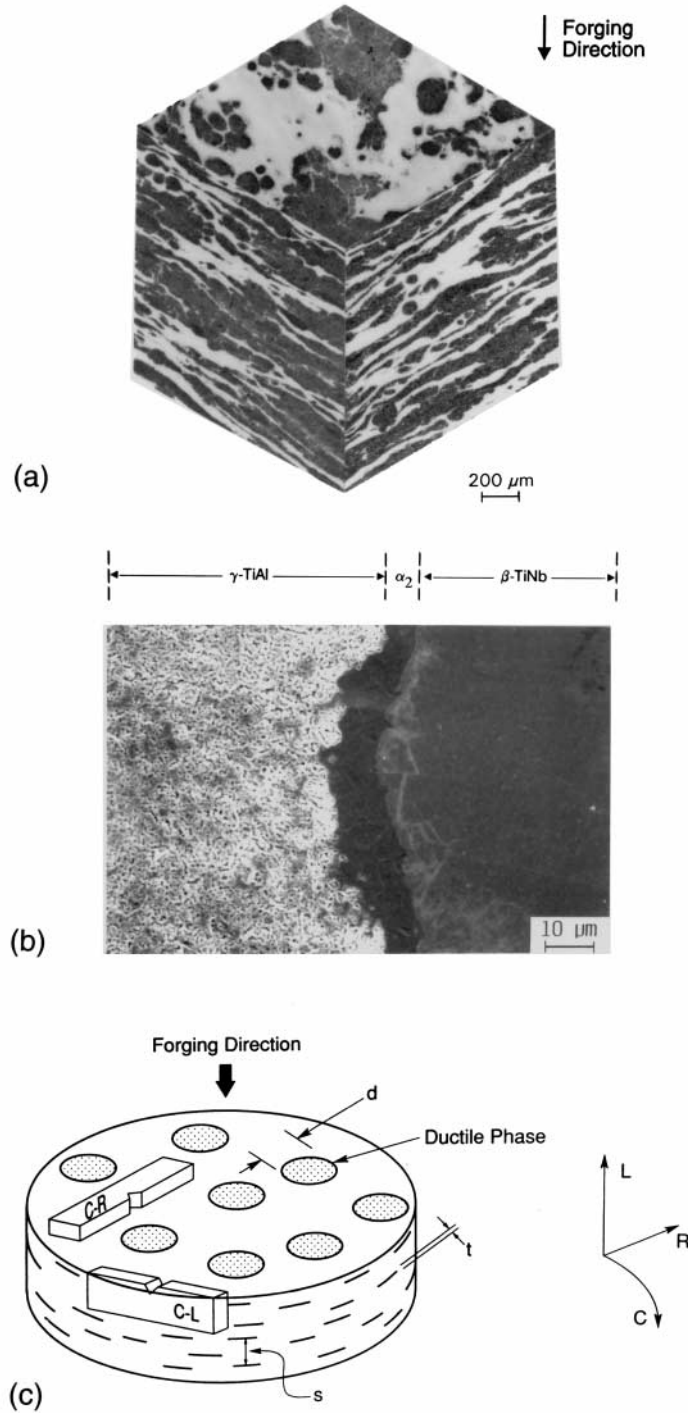


Fig. 1. (a) Three-dimensional optical micrograph of a γ -TiAl composite reinforced with 20 vol.% TiNb particles, (b) scanning electron micrograph of the TiNb/TiAl interface and (c) specimen orientations, C-R (edge) and C-L (face), relative to the composite forging. L, C and R refer to the forging, circumferential and radial directions, respectively.

strongly bonded to TiAl, although the reverse is true under monotonic loading [13].

To date, most observations on the fatigue and fracture properties of ductile-phase toughened γ -TiAl composites pertain to room temperature; very little is known about their monotonic and cyclic crack-growth resistance at elevated temperatures. Since these composites are mainly intended for elevated temperature use up to about 800°C, there is obvious concern whether the presence of the ductile phase will significantly degrade the high-temperature properties of the TiAl alloy. This is of particular concern for TiNb and Nb ductile reinforcements due to the poor oxidation resistance of Nb and Nb-based alloys [14]. Accordingly, the intent of the present study is to examine the crack-growth response and underlying mechanisms associated with high-temperature fatigue and fracture in a 20 vol.% TiNb-reinforced γ -TiAl intermetallic composite at 650 and 800°C in air. Results are compared with data obtained at room temperature and to the behavior in monolithic γ -TiAl, fabricated under identical processing conditions, to discern the degradation in high-temperature properties caused by the addition of TiNb reinforcements.

2. MATERIALS AND EXPERIMENTAL PROCEDURES

2.1. Composite fabrication and microstructure

The ductile-particle reinforced composite was fabricated by mixing -80 mesh γ -TiAl (Ti-55 at.% Al) powder with 20 vol.% of β -TiNb (Ti-33 at.% Nb solid solution) powder of -35 + 50 mesh (nominal size \sim 300–500 μm). The blended powder was hot pressed and forged at 1025°C, producing a pancake-shaped TiNb particle morphology with a nominal aspect ratio of 5:1 and a particle thickness of \sim 40 μm . Unreinforced γ -TiAl was produced by hot pressing the TiAl powder and forging the compact under identical conditions as the composite.

The resultant microstructure, shown in Fig. 1(a), is comprised of a heterogeneous distribution of TiNb islands within a TiAl matrix. Matrix regions of the composite, and the unreinforced γ -TiAl alloy, consist mainly of \sim 2–10 μm sized γ grains with small regions of α_2 -Ti₃Al (ordered-hexagonal DO₁₉ structure) phase. Thermomechanical processing results in a 5–10 μm thick interfacial reaction layer between TiAl and TiNb composed of α_2 +B₂ (ordered b.c.c.) and possibly some ω (B8₂) phase (Fig. 1(b)). The TiNb/TiAl interface is relatively strong at room temperature with virtually no interfacial decohesion; some debonding is seen along the γ/α_2 interface indicating a reaction-layer toughness greater than \sim 330 J/m².

Yield and ultimate tensile strengths for γ -TiAl at 25°C range between 400 and 500 MPa with a tensile elongation of \sim 1.8% [3–5]. The corresponding strength of the TiNb phase was determined from

measurements on the Ti-33 at.% Nb bulk material; these show a yield strength of \sim 430 MPa at 25°C, with no evidence of strain hardening (strain-hardening exponent \sim 0). Deformation in the TiNb phase is thus highly localized such that the measured fracture strain depends strongly on specimen geometry and gauge length. Limited high-temperature tensile data for (γ + α_2)-TiAl + 20 vol.% TiNb composites [15] indicate that they retain their strength up to \sim 800°C; above 800°C, the strength drops drastically concurrent with a large increase in ductility. No plastic elongation was evident in tensile tests on the composites below 800°C; the monolithic alloys, conversely, show limited elongation between room temperature and 800°C.

2.2. Mechanical testing

Fatigue-crack growth behavior in the TiNb/TiAl composite and unreinforced γ -TiAl was examined under tension-tension loading, using 25 mm wide, 4.5 mm thick, compact tension C(T) specimens in the edge (C-R) orientation, where particle edges are oriented normal to the crack plane (Fig. 1(c)). All specimens were fatigue precracked under alternating tensile loads at the test temperature; pure γ -TiAl samples were additionally fabricated with a wedge-shaped notch to aid this procedure. Tests were performed at 650 and 800°C in air using automated servo-hydraulic testing machines operating under stress-intensity (K) control, with crack length being continuously monitored, to a resolution of \pm 100 μm , using load-line displacement-based compliance techniques [16]. Compliance values were verified by periodic *in situ* crack length measurements on the specimen surface, imaged through a sapphire-window port installed on the furnace, using a high-resolution optical telescope equipped with a video camera, image capturing, storage and image processing capabilities.

Cyclic loads were applied at a constant load ratio, $R = K_{\text{min}}/K_{\text{max}}$, of 0.1 and a frequency of 25 Hz (sine wave), with the far-field (applied) stress-intensity range, $\Delta K = K_{\text{max}} - K_{\text{min}}$, varied using an exponential load-shedding scheme with the K -gradient set to \pm 0.1/mm [17]. Using such procedures, crack-growth rates per cycle (da/dN) were measured between 10^{-6} and 10^{-12} m/cycle. The ΔK level corresponding to the slowest growth rate, $da/dN \leq 10^{-12}$ m/cycle, was operationally defined as the fatigue threshold (ΔK_{TH}) below which no appreciable crack growth is apparent.

Fracture toughness properties were evaluated in terms of resistance curves, i.e. by measuring fracture resistance (K_{R}) as a function of crack extension (Δa). Fatigue tested samples were monotonically loaded, under displacement control, until crack growth could be initiated. Crack initiation was detected either from any deviation from linearity or a sudden load drop on the load-displacement record. In addition, the event was also monitored

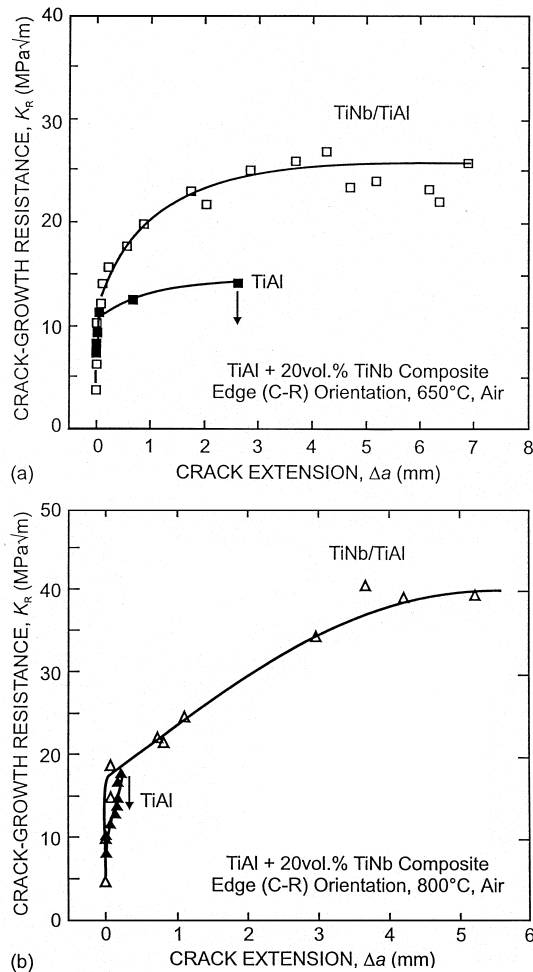


Fig. 2. Resistance-curve behavior of TiAl + 20 vol.% TiNb composite under monotonic loading at (a) 650°C and (b) 800°C in air, in the edge (C-R) orientation, compared to the corresponding behavior in unreinforced γ -TiAl. Vertical arrow indicates point of catastrophic failure.

by direct observation using the high-resolution optical telescope. Following crack initiation, loads were reduced by $\sim 10\%$ to stabilize crack extension and record load, crack length and other relevant observations; loads were again increased to further

advance the crack, and the process was repeated until final fracture of the sample. Applied load and crack length values were used to calculate the stress intensities (K_R), consistent with procedures outlined in ASTM Standard E-399 [16]. Results are expressed in terms of the critical stress intensity at crack initiation (K_i) and the maximum stress intensity at steady state on the plateau of the R-curve (K_{ss}).

Fracture surfaces and profiles of crack paths in the loading plane were imaged using optical and scanning electron microscopy (SEM). In addition, crack/particle interactions were digitally recorded *in situ* using the image grabbing and storage facilities of the telescope/video-camera system.

3. RESULTS AND DISCUSSION

3.1. Fracture toughness behavior

3.1.1. Crack growth at 650 and 800°C. The crack-growth response of the TiNb/TiAl composite and unreinforced TiAl to monotonically increasing loads at 650 and 800°C is shown for the edge (C-R) orientation in Fig. 2(a) and (b), respectively; data are summarized in Table 1. It is clear that the presence of TiNb particles enhances the fracture resistance of TiAl, both at 650 and 800°C, similar to previously reported results at room temperature [11–13]. The onset of cracking in the composite was seen at $K_i = \sim 14$ and ~ 18 MPa $m^{1/2}$ at 650 and 800°C, respectively; further crack growth occurred in stable fashion at progressively higher stress intensities. At 650°C, the resulting R-curve displayed a maximum (“plateau”) toughness of $K_{ss} = \sim 25$ MPa $m^{1/2}$ after ~ 4 mm of crack extension [Fig. 2(a)]; at 800°C, the plateau toughness was considerably higher, with $K_{ss} = \sim 40$ MPa $m^{1/2}$ [Fig. 2(b)] after about 4 mm of crack growth.

Corresponding failures in monolithic γ -TiAl at 800°C occurred catastrophically, without significant stable crack growth prior to final failure; however, gross plastic deformation was apparent on the surface at the crack tip before fracture. Stable crack growth was apparent in TiAl at 650°C, as indicated by the shallow R-curve in Fig. 2(a); cracking

Table 1. Summary of monotonic and cyclic crack-growth properties ($R = 0.1$) of γ -TiAl composites (C-R orientation)

Temperature	Fracture toughness (MPa $m^{1/2}$) [†]	Fatigue threshold, ΔK_{TH} (MPa $m^{1/2}$)	Fatigue threshold, $K_{max,TH}$ (MPa $m^{1/2}$)	Exponent, m [‡]	Constant, C [§]
γ -TiAl					
25°C	8	5.8	6.4	29.4	9.7×10^{-31}
650°C	11–14	4.2	4.6	4.6	2.0×10^{-11}
800°C	12–18	5.5	6.1	6.3	3.5×10^{-13}
γ -TiAl + 20% TiNb					
25°C	16–40	5.0	5.5	9.6	2.0×10^{-13}
650°C	14–27	4.5	5.0	7.6	7.6×10^{-14}
800°C	19–40	4.9	5.4	6.9	1.8×10^{-10}
β -TiNb					
25°C	12–57	1.7	1.9	4.6	3.0×10^{-11}

[†]Range represents the initiation (K_i) and maximum (K_{ss}) toughness values on the R-curve.

[‡]Taken for crack-growth rates in the intermediate growth-rate region ($\sim 10^{-8}$ – 10^{-5} m/cycle).

[§]In Paris relationship: $da/dN = C\Delta K^m$ —units: m/cycle (MPa $m^{1/2}$)^{-m}.

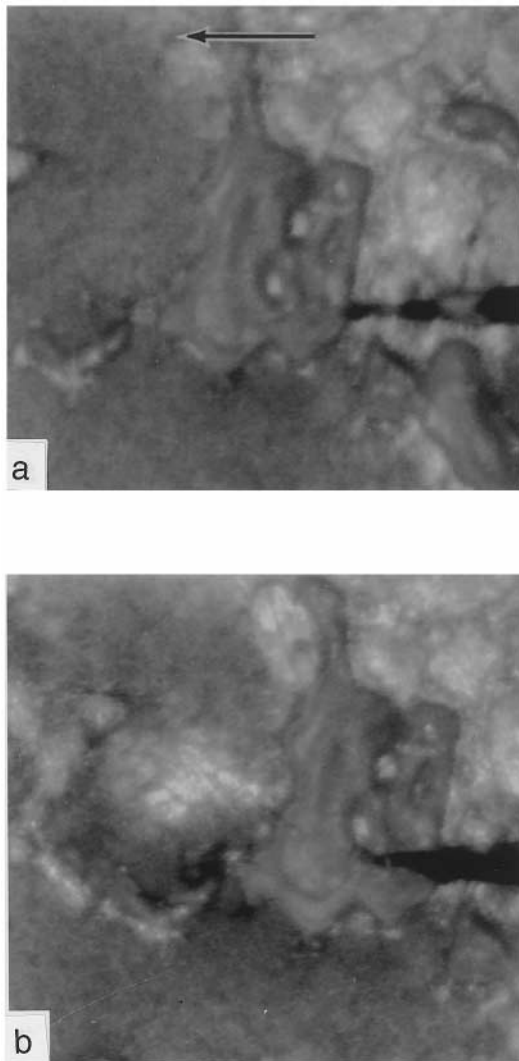


Fig. 3. *In situ* optical telescopic images of a sequence of crack/particle interactions observed during monotonic loading of the TiNb/TiAl composite at 800°C in air. Arrow indicates the direction of crack growth.

initiated at $\sim 11 \text{ MPa m}^{1/2}$ and final failure occurred at $\sim 14 \text{ MPa m}^{1/2}$ after about 3 mm of crack growth. Failures in unreinforced TiAl at room temperature also occurred catastrophically at a K_{Ic} value of $\sim 8 \text{ MPa m}^{1/2}$, but showed no evidence of plastic deformation on the specimen surface.

From Fig. 2 it is apparent that the addition of ductile TiNb phase increases both crack-initiation and crack-growth (R-curve) toughnesses, relative to TiAl, at high temperatures, although the influence on crack-initiation toughness is relatively small at elevated temperatures; measured K_i values in the TiNb/TiAl composite are comparable to K_c values of monolithic TiAl at 650 and 800°C. Crack advance at high temperatures is associated with crack/particle interactions similar to those noted at room temperature [13]. Although quality is lacking, *in situ* telescopic images of crack extension were

taken at 800°C (Fig. 3). This figure illustrates a typical sequence where the advancing crack arrests near a ductile TiNb particle [Fig. 3(a)], followed by crack-tip blunting and renucleation in the matrix ahead of the particle [Fig. 3(b)]. One difference, however, is that the severity of crack-tip blunting and associated crack-opening displacements are significantly greater at 800°C than at ambient temperature [13], due to the large increase in ductility and resultant crack-tip plasticity above the ductile-to-brittle transition temperature (DBTT, of $\sim 700^\circ\text{C}$ [18]) for γ -TiAl.

Crack blunting and renucleation phenomena, induced by the presence of TiNb reinforcements in the microstructure, undoubtedly provide major contributions to crack-initiation toughness of the composite at room temperature [13]. The effectiveness of such mechanisms at high temperatures, however, is unclear; crack-tip blunting due to plastic deformation appears to be more prominent. As the crack extends further, recurrent crack arrest near TiNb particles, crack-tip blunting and microcrack nucleation ahead of the main crack tip, above or below the principal crack plane, results in the formation of unbroken TiNb ligaments and overlapping TiAl ligaments in the crack wake. Bridging tractions provided by these intact ligaments contribute to the rising portion of the R-curve and hence to crack-growth toughening before the ultimate rupture of TiNb particles at large crack-opening displacements.

The resulting fracture surfaces in composites tested at high temperatures under monotonic loading showed that TiNb particles ruptured transgranularly by microvoid coalescence, as evidenced by large dimples on the fracture surface [Fig. 4(d)]. Features are similar to those at 25°C, excepting that the size of dimples in the TiNb phase is significantly greater at 800°C ($1\text{--}5 \mu\text{m}$ at 25°C vs $10\text{--}40 \mu\text{m}$ at 800°C). The γ -TiAl matrix, conversely, failed by complete intergranular fracture at 800°C, above the DBTT [Fig. 4(c)], both in monolithic and composite form, and by a mixed transgranular cleavage and intergranular fracture at 25 and 650°C [11,13], although there was a larger proportion of intergranular fracture at 650°C. Secondary cracking was also apparent along the matrix/reaction layer interface [Fig. 4(a) and (b)] suggestive of strong bonding between the TiAl and TiNb constituent phases, even at elevated temperatures.

3.1.2. Influence of temperature. The temperature dependence of fracture toughness in the TiNb/TiAl composite is plotted in Fig. 5(a); results for unreinforced γ -TiAl are also shown in Fig. 5(b) for comparison. It is apparent that pure γ -TiAl shows a modest elevation in toughness from $\sim 8 \text{ MPa m}^{1/2}$ at 25°C to about $18 \text{ MPa m}^{1/2}$ at 800°C, that is most likely associated with increased ductility above the DBTT [3,4,18]. At 650°C, just below the DBTT, toughness is intermediate to the behavior at 25 and

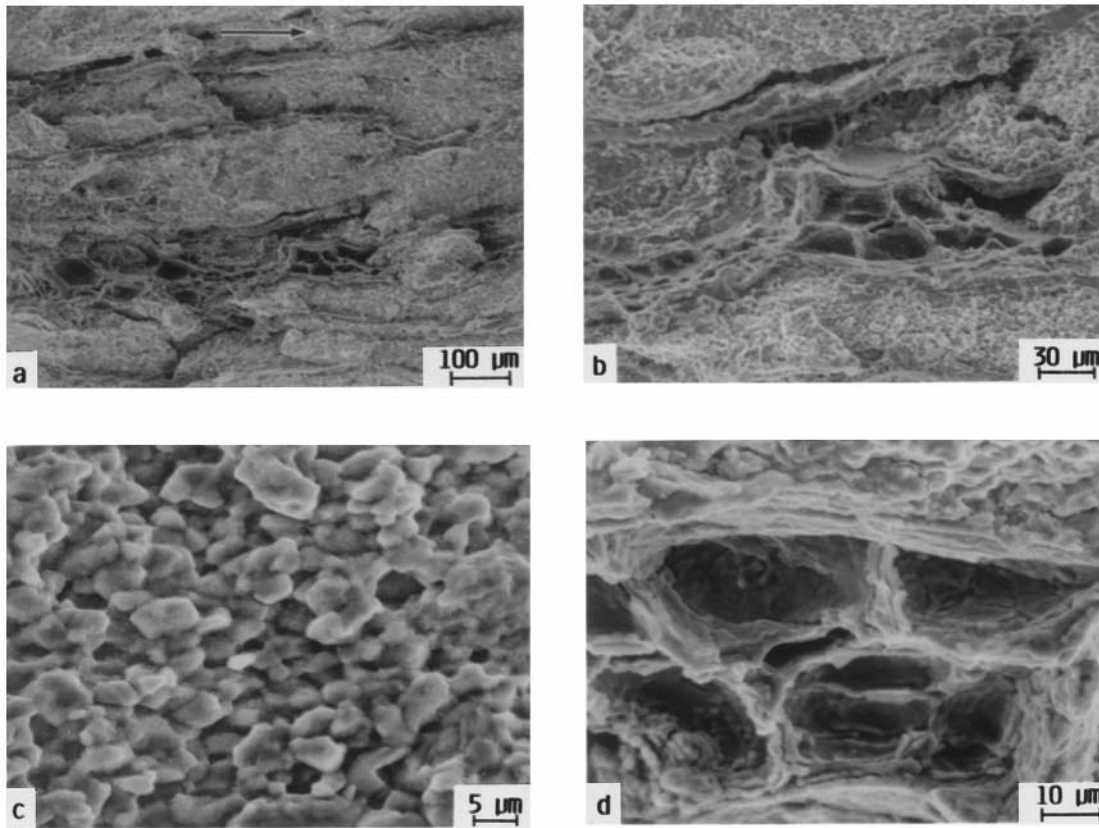


Fig. 4. SEM micrographs of fracture surfaces in the TiNb/TiAl composite tested under monotonic loading in air at 800°C. Micrographs (c) and (d) are high magnification images of the TiAl matrix and TiNb particle regions of the composite. Arrow indicates the direction of crack growth.

800°C; however, as noted previously, stable crack growth is observed at 650°C characterized by a shallow R-curve. Corresponding sample surfaces at 650°C exhibit large deformation zones surrounding the crack (Fig. 6); at 800°C, plastic deformation was severely localized at the crack tip and failures were catastrophic. Reasons for such behavior at 650°C are not clear, although similar results have been obtained in other two-phase ($\gamma + \alpha_2$)-TiAl microstructures [19–21]. Increased propensity for crack-tip deformation by twinning at high temperatures below the DBTT is one plausible explanation.

The composite, on the other hand, shows almost no change in fracture resistance with increase in temperature between 25 and 800°C, although there is some degradation in toughness at 650°C at crack extensions beyond ~ 2 mm. This behavior is presumed to result from a mutual competition between several mechanisms, involving an increase crack-initiation toughness due to improved ductility of γ -TiAl at higher temperatures, which is offset by a concurrent reduction in crack-growth toughness resulting from the lower strength (or bridging ligament tractions) provided by the TiNb particles.

To validate these notions, the crack-growth behavior under monotonic loading was evaluated in terms of simple models for bridging, based on an

energy approach [22] (that accounts for toughening in terms of an increase in fracture energy due to the addition of ductile particles) or a superposition approach [23] (where the toughening increment is estimated from the bridging tractions provided by intact ligaments in the crack wake). Tensile tests were performed on the bulk reinforcement material, i.e. TiNb sheet samples, at 650 and 800°C to measure the relevant parameters, namely the yield strength, modulus and work of fracture of the reinforcement. Results are summarized in Table 2. Also shown are the predictions from the two models [22, 23]; steady-state plateau toughness values based on the energy approach show a closer correspondence to experimental values. However, both models correctly predict the temperature dependence of toughness in the TiNb/TiAl composite further confirming the reduced efficacy of ductile-phase bridging from TiNb particles at high temperatures.

Overall, however, it is clear that the addition of ductile TiNb reinforcements does not seriously compromise the high-temperature fracture properties of γ -TiAl at the temperatures of intended use. In fact, the TiNb particles are effective in intercepting crack advance in the composite even at 800°C and lead to uncracked ligament bridging in the crack wake.

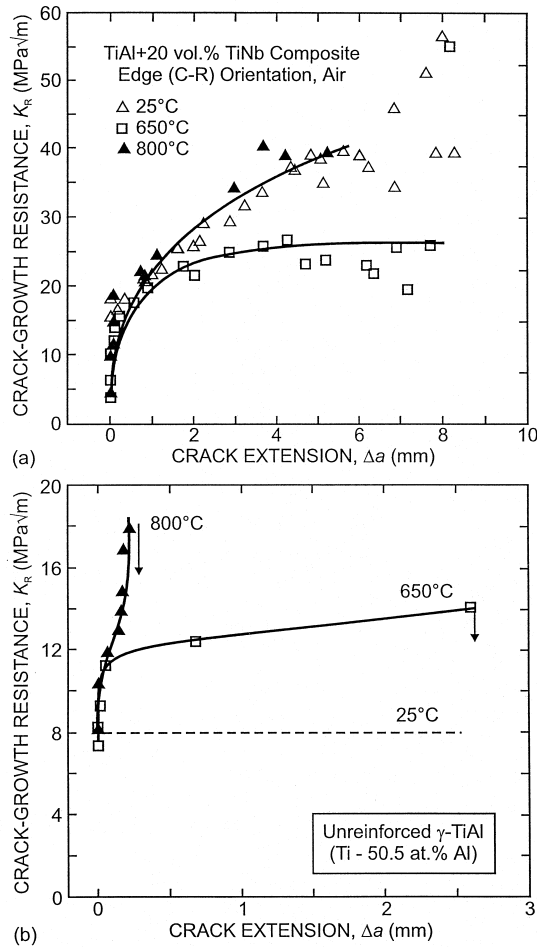


Fig. 5. Effect of temperature on the monotonic fracture resistance of TiAl + 20 vol.% TiNb composite in air. Note that the TiNb-reinforced composite retains its superior toughness over unreinforced γ -TiAl at temperatures up to 800°C. Vertical arrow indicates point of catastrophic fracture.

However, the degree of toughening associated with TiNb particles is significantly lower compared to results at room temperature due to a reduction in the bridging tractions (or effective strength) provided by TiNb reinforcements from lower yield stress. The decrease is offset by concurrent improvements in crack-initiation toughness of the TiAl matrix at elevated temperatures, specifically above the DBTT. Accordingly, the TiNb reinforcements do not appear to have a detrimental effect on the high-temperature fracture properties of TiAl alloys.

However, such effective toughening by TiNb reinforcements may not be realized over extended periods of time at elevated temperatures if the TiNb degrades from environmental attack in unprotected atmospheres due to the low oxidation resistance of Nb-bearing alloys. Indeed, severe oxidation of TiNb particles was apparent on specimen surfaces after fatigue testing in air for only 2–3 days at elevated temperatures. The extent of oxidation was sig-

nificantly greater in the TiNb phase than in the TiAl matrix, with TiNb particles seen initially to bulge followed by cracking in the oxide scales. Clearly, if alloys containing TiNb reinforcements are to be seriously contemplated for service use in structural applications, the development of suitable protective coatings on surfaces would be essential to minimize such environmental degradation.

3.2. Fatigue-crack propagation behavior

Fatigue-crack growth results for the β -TiNb/ γ -TiAl composite (C-R orientation) at 650 and 800°C in air are plotted in Fig. 7(a) and (b), respectively, together with equivalent data for unreinforced γ -TiAl. Behavior is again somewhat similar to that observed at room temperature [13]. In both the monolithic and composite alloys, cracks are observed to propagate subcritically at ΔK levels between ~ 4 and $10 \text{ MPa m}^{1/2}$, well below the stress intensities of ~ 12 – $18 \text{ MPa m}^{1/2}$ needed to initiate crack growth under monotonic loads. This highlights the fact that subcritical crack propagation by fatigue remains an important damage mechanism in TiAl alloys at high temperatures.

Specifically at 800°C, fatigue-crack growth rates in the composite are slightly faster, yet still comparable to, rates in unreinforced γ -TiAl; the largest difference is at near-threshold stress intensities, where the fatigue threshold for the composite ($\Delta K_{TH} = \sim 4.9 \text{ MPa m}^{1/2}$) is $\sim 20\%$ lower than in the unreinforced matrix (Table 1). At 650°C, fatigue-crack growth rates between the monolithic alloy and composite are equivalent. Thus, in contrast to the behavior under monotonic loading, the addition of TiNb reinforcements does not significantly enhance the crack-growth resistance under cyclic loads, and at 800°C marginally accelerates fatigue-crack propagation, at least for the edge-oriented composites tested in this study.

Such behavior is consistent with *in situ* telescopic observations of cyclic crack growth which indicate that TiNb-particle bridging in the crack wake was not apparent in the TiNb/TiAl composite at elevated temperatures. Figure 8 illustrates a typical sequence of digital images taken during cyclic crack growth at 800°C under decreasing ΔK conditions between 6 and $7 \text{ MPa m}^{1/2}$. Akin to observations made previously for cyclic crack growth at room temperature [13], the fatigue crack advances into the ductile TiNb particle (marked by an arrow) without noticeable interaction, which subsequently fails along with the matrix. Corresponding crack profiles were linear with smaller crack-opening displacements than under monotonic loading (Fig. 3). In addition, the potency of any crack-bridging effects during cyclic loading was assessed by comparing estimates of the crack length derived from load-line compliance measurements with those measured using the optical telescope [24]. Close agreement (to within a few percent) was obtained

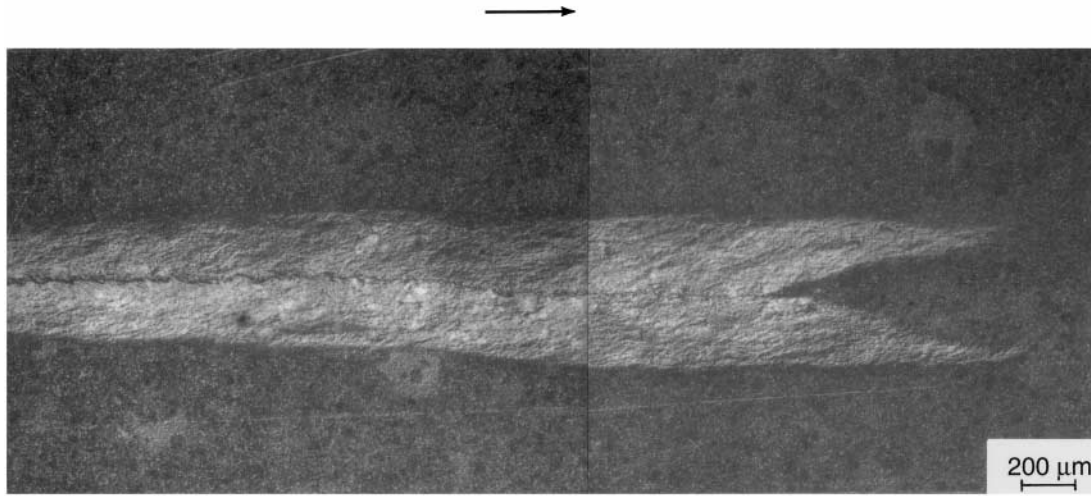


Fig. 6. SEM micrograph of the crack profile on the unreinforced γ -TiAl specimen surface after crack growth under monotonic loading at 650°C. Note the long deformation zones surrounding the crack profile. Arrow indicates direction of crack growth.

between these two crack-length measurements, suggesting that crack bridging effects by the ductile phase during fatigue were minimal.

3.2.1. Effect of temperature. Fatigue-crack growth rates in γ -TiAl and TiNb/TiAl at various temperatures are compared in Fig. 9(a) and (b). In the near-threshold region ($da/dN < 10^{-8}$ m/cycle), growth rates at a fixed ΔK in either material vary by 1–2 orders of magnitude between 25 and 800°C; smaller differences are seen at higher growth rates. However, the variation in fatigue resistance with temperature is not linear; crack-propagation rates are faster, and corresponding fatigue threshold values lower, at 650°C compared to either 800°C or room temperature. Fortunately, over the majority of crack-growth behavior (i.e. $\sim 10^{-8}$ – $> 10^{-5}$ m/cycle), these differences in fatigue resistance between 25, 650 and 800°C are not large (less than an order of magnitude variation in growth rates). Accord-

ingly, it can be concluded that reinforcement with TiNb particles to enhance room-temperature toughness does not severely reduce the high-temperature fatigue resistance of γ -TiAl.

Other features on da/dN – ΔK curves for γ -TiAl and TiNb/TiAl are typical of those seen in many metallic materials, namely a near-threshold region below $\sim 10^{-8}$ m/cycle (region I), where the dependency of crack-growth rate on the applied ΔK is high, and an intermediate region between $\sim 10^{-8}$ and $\sim 10^{-5}$ m/cycle (region II), where this dependency is less severe. However, in contrast to the behavior in metals, the da/dN – ΔK dependence is much higher in the intermetallic composite. For example, considering region II in the composite, the exponent m in the empirical Paris power-law relation ($da/dN = C\Delta K^m$), which is often used to describe this region, is between ~ 7 and 10 (Table 1). Although m decreases with increasing temperature, these values

Table 2. Modeling calculations for the temperature dependence of fracture toughness in the TiNb/TiAl composite

Temperature (°C)	25	650	800
Measured composite plateau toughness (MPa m ^{1/2})	40	25	40
Measured yield strength of TiNb (MPa)	430	120	99
Measured work of fracture for TiNb, W (kJ/m ²)	54.2	30.5	44.3
Young's modulus for TiNb, E_{TiNb} (GPa)	75	22.1	9.2
Young's modulus for TiAl, E_{TiAl} (GPa)	177	149	133.8
Composite modulus, E_{comp} (GPa)†	156.6	123.6	108.9
Crack-initiation toughness, $K_{\text{i-TiAl}}$ (MPa m ^{1/2})	8	9.3	10.3
Plateau toughness of pure γ -TiAl, $K_{\text{c-TiAl}}$ (MPa m ^{1/2})	8	14.1	17.6
Composite-initiation toughness, K_{tip} (MPa m ^{1/2})	17.3	12	18.8
	<i>Energy approach</i>		
Energy increase, $\Delta G_{\text{c}} = fW$ (J/m ²)‡	10.8	6.1	8.8
Predicted toughness, $K_{\text{ssb}} = \sqrt{K_{\text{tip}}^2 + E_{\text{comp}}\Delta G_{\text{c}}}$	44.7	30.0	36.3
	<i>Superposition approach</i>		
Bridging zone length, L_{ssb} (m)	0.006	0.003	0.004
Bridging ligament stresses, σ_{y} (MPa)§	430	120	99
Shielding from bridging, $\Delta K_{\text{b}} = 2f\sigma_{\text{y}}\sqrt{(2L_{\text{ssb}}/\pi)}$	10.6	2.1	2.0
Composite toughness, $K_{\text{ssb}} = K_{\text{tip}} + \Delta K_{\text{b}}$ (MPa m ^{1/2})	27.9	14.1	20.8

†Composite modulus based on rule of mixtures.

‡Based on a nominal volume fraction, $f = 0.2$.

§Tensions in the bridging zone, $\sigma(x) = f\sigma_{\text{y}}$, and are assumed to be uniform in the wake.

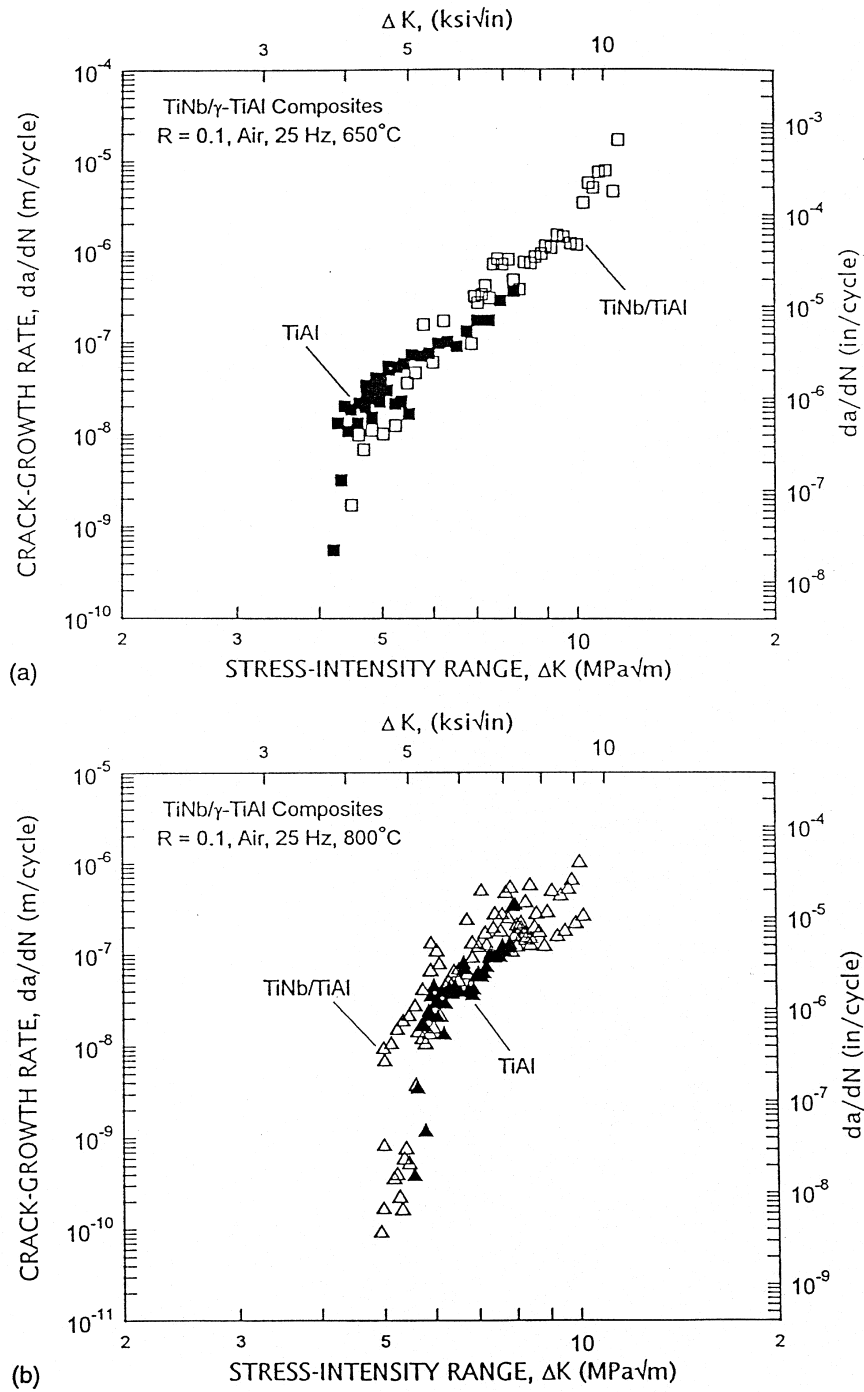


Fig. 7. Fatigue-crack propagation behavior in the TiAl + 20 vol.% TiNb composite (edge or C-R orientation) compared to monolithic $\gamma\text{-TiAl}$ at (a) 650°C and (b) 800°C in air. Test results are for $R = 0.1$ and a frequency of 25 Hz.

are large compared to those typically found in metals over this regime, where $m = \sim 2-4$.

This dependence is stronger for unreinforced $\gamma\text{-TiAl}$, which at room temperature displays limited damage tolerance with a very steep $da/dN-\Delta K$ curve ($m = \sim 30$) and little distinction between the near-threshold and intermediate regimes of crack growth. At 800°C , TiAl does exhibit a small inter-

mediate growth-rate region on the $da/dN-\Delta K$ curve (with $m = \sim 6$), which is most probably associated with the improved ductility of the gamma structure at temperatures above the DBTT. The anomalous dependence of fatigue resistance on temperature dependence, characterized by faster crack-growth rates at 650°C compared to ambient and 800°C , is more clearly apparent compared to the composite.

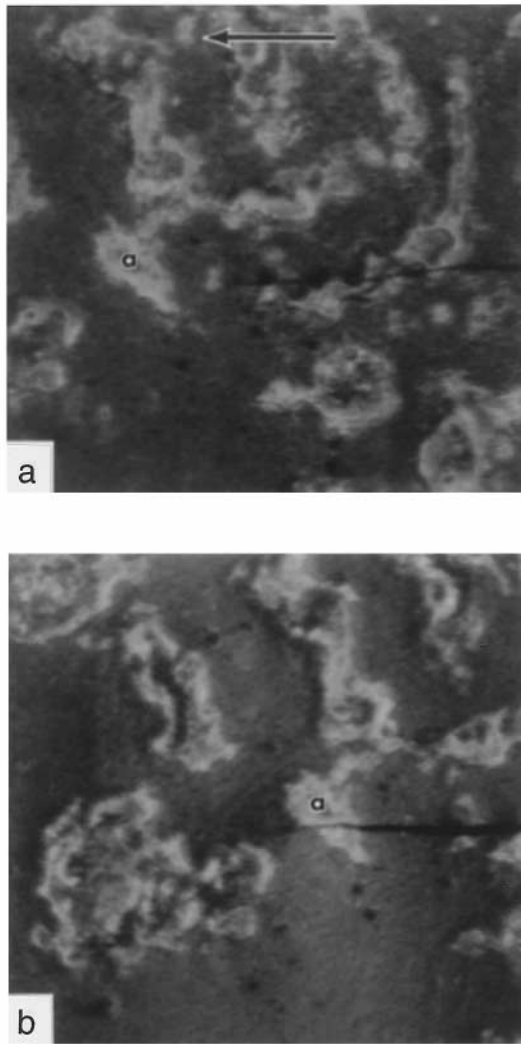


Fig. 8. *In situ* optical telescopic images of a sequence of crack/particle interactions observed during cyclic loading in the TiNb/TiAl composite at 800°C in air. Note that the crack traverses the particles (marked (a)) without significant interaction. Arrow indicates the direction of crack growth.

Such trends have been reported in other studies on TiAl-based alloys reasons for which are not fully clear. Large improvements in ductility of γ -TiAl at 800°C above the DBTT [19], shielding from oxide wedging in the crack wake at 800°C [20], and pronounced environmental effects in the 600–650°C range, just below the DBTT [21], have all been proposed as possible explanations to account for this anomalous variation in fatigue properties with temperature.

3.2.2. Cyclic crack-growth mechanisms. Fatigue fracture surfaces in the composite at 800°C were quite smooth (Fig. 10) compared to the very rough topography seen after monotonic failure (Fig. 4). Despite oxidation on the surfaces, the TiNb particles can be observed to fail by transgranular shear, similar to the behavior at room

temperature [13], and is particularly evident at intermediate to high growth rates (Fig. 10(a) and (c)). The transgranular nature of fatigue fracture in the TiNb phase is not as clear, however, at the slower growth rates close to the threshold (Fig. 10(b) and (d)); here, oxidation of the TiNb phase is more prevalent with the crack extending by the cracking of the oxide. Fatigue failure in the γ -TiAl matrix at 800°C, conversely, occurs by transgranular cleavage mixed with intergranular modes; this is to be compared with the 100% intergranular failure mode observed under monotonic loading (Fig. 4(c)).

It may be inferred from the above observations that the suppression of crack-tip shielding from TiNb-ligament bridging under cyclic loading is a primary cause for subcritical fatigue-crack growth in TiNb/TiAl composites at elevated temperatures. As reported previously for room-temperature behavior [13], and unlike toughening under monotonic loads, fatigue-crack growth rates in the composite often exceed those in unreinforced γ -TiAl because the advancing crack is unable to establish a significant bridging zone under cyclic loading. This is due to the fact that fatigue cracks extend at much lower stress intensities, and hence with smaller crack-tip opening displacements, than under monotonic loads, and most importantly because the TiNb particle bridges that do form simply fail prematurely by fatigue.

The notion of fatigue-crack growth promoted by the cycle-dependent suppression of shielding in the crack wake is similar to mechanisms of fatigue-crack growth in other low-ductility materials, specifically the room-temperature behavior of ceramics [25–27]. For example, ceramics such as alumina and silicon nitride, which display (extrinsic R-curve) toughening from crack bridging via interlocking grains, are susceptible to fatigue-crack growth from degradation of such bridging under cyclic loads [27]. There is one significant difference though for fatigue-crack growth in intermetallics. At ambient temperatures, there is no intrinsic fatigue damage mechanism in ceramics—the crack tip advances by an identical mechanism under monotonic and cyclic loads; at a given stress intensity, fatigue cracks simply grow faster due to the cyclic suppression in shielding behind the crack tip. Accordingly, the value of maximum stress intensity at the fatigue threshold, $K_{\max, TH}$, is comparable with the crack-initiation toughness, K_i , at the start of the R-curve ($K_{\max, TH} \sim K_i$). In the present γ -TiAl alloys, conversely, fatigue-crack growth is seen at stress-intensity levels far below the crack-initiation toughness, specifically $K_{\max, TH} = \sim 0.25\text{--}0.4K_i$ (Table 1). This implies that in addition to the *extrinsic* effect of degradation in shielding under cyclic loading, there are *intrinsic* microstructural damage mechanisms uniquely associated with fatigue failure in intermetallics. In this respect, γ -TiAl alloys behave like metallic

materials, where microstructural damage and crack advance is associated with dislocation activity and resultant alternating blunting and resharpening of the crack tip during the fatigue cycle [28,29]. However, the limited crack-tip plasticity and consequently lower toughness in intermetallics render the stage II crack-growth region to be far more restrictive; accordingly, the dependence of da/dN on applied ΔK will be much stronger over a larger range of crack-growth rates

than in corresponding metallic high-temperature materials (but lower than in ceramics).

Such a marked dependency of growth rates on stress intensity implies that the structural life of a component will be strongly sensitive to applied stress and crack size. Accordingly, the structural application of such intermetallic alloys may well be hampered by difficulties in design and life-prediction methodologies. Using conventional damage-tolerant design philosophies, the life spent in crack propa-

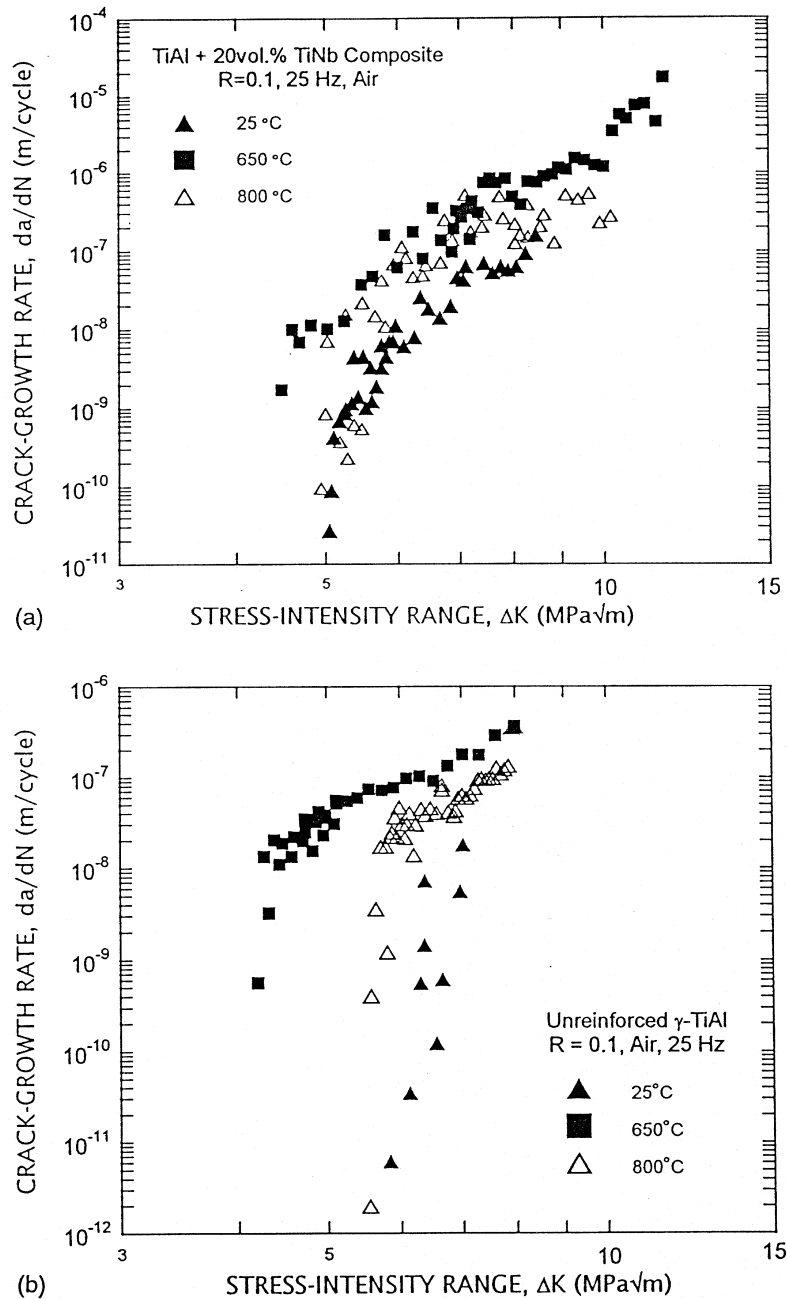


Fig. 9. Effect of temperature on fatigue-crack growth rates in (a) TiAl + 20 vol.% TiNb composite (edge orientation), and (b) unreinforced γ -TiAl, in air. Note that at a given ΔK , growth rates in the composite are fastest at 650°C compared to the behavior at either room temperature or 800°C. Test results are with $R = 0.1$ and a frequency of 25 Hz.

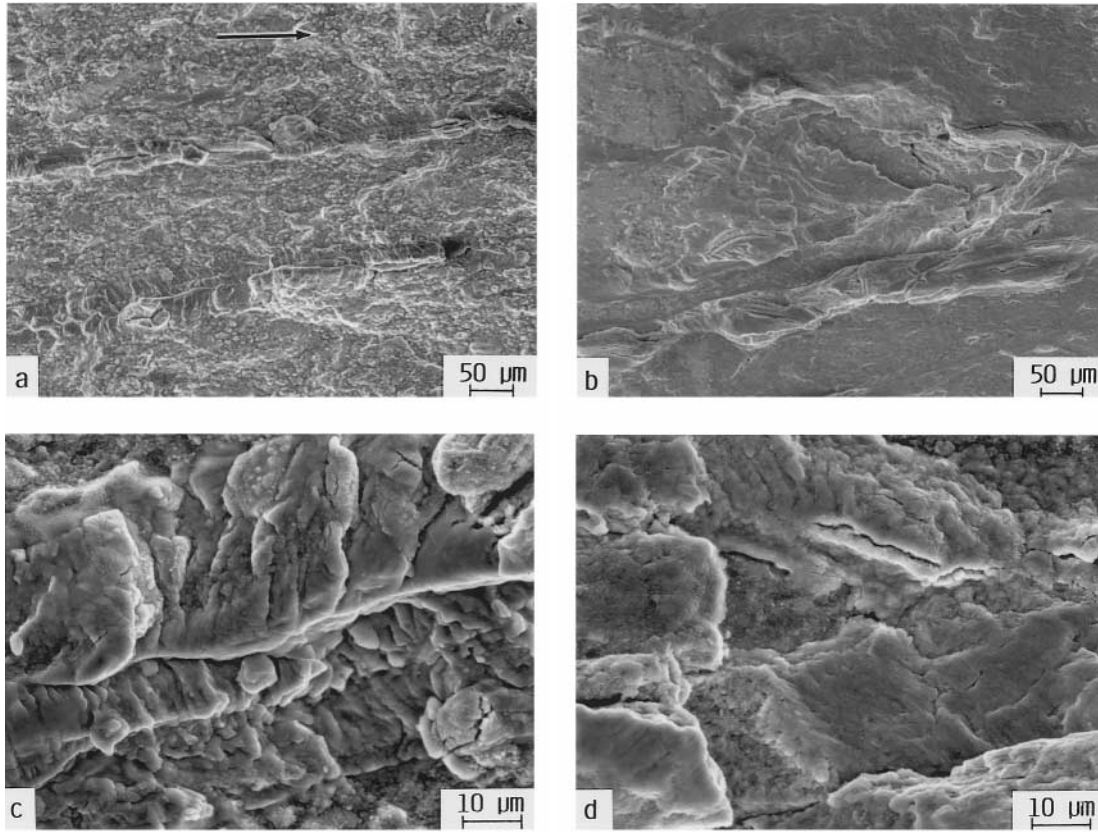


Fig. 10. SEM micrographs at various magnifications of the fracture surfaces in TiNb/TiAl composite tested under cyclic loading at 800°C in air (a, c) at intermediate ($\Delta K = 7 \text{ MPa m}^{1/2}$), and (b, d) at near-threshold levels ($\Delta K = 5.5 \text{ MPa m}^{1/2}$). Note the extensive oxidation of TiNb particles, especially at near-threshold stress intensities. Arrow indicates the crack-growth direction.

gation in γ -TiAl alloys will be extremely limited due to the steepness of the da/dN - ΔK curves; this suggests that design approaches based on the fatigue threshold for no crack growth may be better suited for these materials. While acceptable in principle, this places greater emphasis on the characterization of the fatigue behavior of small cracks in these alloys if an accurate description of near-threshold behavior is to be achieved; such small-crack behavior, however, has not been characterized to date in ductile-phase toughened γ -TiAl alloys.

3.3. Concluding remarks

In general, this study has shown that composite reinforcement with ductile TiNb particles to enhance room-temperature toughness of γ -TiAl does not adversely affect the high-temperature fatigue and fracture resistance of the intermetallic alloy. Although properties are somewhat degraded, particularly at 650°C, fracture toughness, fatigue-crack propagation rates and fatigue thresholds are all comparable to values measured at room temperature. However, as noted previously at 25°C [13], the toughening imparted by the presence of ductile phases is generally not realized under cyclic loading due to premature fatigue failure of the ductile brid-

ging ligaments. Moreover, the presence of the TiNb phase naturally could cause problems during prolonged thermal exposure due to the environmental sensitivity and low oxidation resistance.

With respect to properties at 650°C, the measured variation in crack-growth rates in TiNb/ γ -TiAl with temperature may appear unusual since it is generally accepted that resistance to crack growth should monotonically decrease with temperature. In the absence of significant creep, environmental effects and/or microstructural instabilities, this is often attributed to an increase in crack-tip opening displacements (a measure of cyclic crack-tip damage governing crack-growth increment per cycle), from reductions in yield strength and elastic modulus with increasing temperature. The occurrence of phase transformations or fracture-mode transitions in a material could clearly alter this trend. In TiAl and its alloys the anomaly appears to result from the fact that brittle-to-ductile transition in the γ -phase occurs above $\sim 700^\circ\text{C}$ (factors such as alloying and strain rate will affect this temperature). For this reason, with increase in temperature at a given stress intensity, growth rates are expected to be faster at 650°C compared to room temperature; however, at 800°C above the DBTT, the large increase

in ductility and ease of plastic deformation and enhanced oxide-induced crack closure and blunting acts to improve the resistance to crack growth. Indeed, such behavior is not uncommon and has been reported in conventional titanium alloys [30], Fe-Si alloys [31], and other dual-phase TiAl intermetallics [19-21].

4. CONCLUSIONS

Based on an experimental study of the fracture toughness and fatigue-crack propagation resistance of β -TiNb ductile-particle toughened, γ -TiAl intermetallic-matrix composites at elevated temperatures up to 800°C, and through comparison to previous results obtained at room temperature [13,15], the following conclusions can be made:

1. The presence of the TiNb ductile phase enhances the fracture toughness of γ -TiAl at 800°C; similar to the behavior at room temperature, the composite shows rising R-curve behavior with a (steady-state) toughness increase from ~ 12 to 40 MPa m^{1/2}.
2. Such toughening at elevated temperatures is also associated with crack trapping, renucleation and resultant formation of intact TiNb bridging zones in the crack wake, although their efficacy was significantly lower relative to behavior at room temperature. Improved crack-initiation toughness at high temperatures is primarily associated with intrinsic changes in crack-tip deformation, possibly from twinning at 650°C and plasticity at 800°C, above the DBTT for TiAl.
3. Ductile-phase toughening from TiNb reinforcements is not realized under cyclic loading at 800°C as premature fatigue failure of ductile particles prevents the formation of a significant crack-bridging zone. Indeed, fatigue-crack growth rates in the C-R orientation are marginally faster in the TiNb/ γ -TiAl composite relative to unreinforced γ -TiAl. However, at a given ΔK level, growth rates in the composite are less than an order of magnitude faster at 800°C than at room temperature.
4. Effect of temperature on the toughness and fatigue-crack propagation resistance is somewhat anomalous in TiNb/ γ -TiAl and pure γ -TiAl in that properties are worse at 650°C than at either room temperature or 800°C. Although the effect is not large (growth rates at a fixed ΔK are 1-2 orders of magnitude faster at 650°C than at 25°C), it is believed to result from the occurrence of the ductile-to-brittle transition in γ -TiAl at approximately 700°C.
5. Overall, the incorporation of ductile TiNb particles to provide a source of room-temperature toughness in γ -TiAl does not appear to compromise the fracture and fatigue-crack growth properties of the intermetallic compound at

temperatures up to 800°C. However, the long-term thermal stability of the composite would clearly be questionable in oxidizing atmospheres due to the environmental sensitivity of the TiNb ductile phase.

Acknowledgements—This work was supported by the U.S. Air Force Office of Scientific Research under Grant No. F49620-93-1-0107, with C. H. Ward as program manager. Thanks are due to C. H. Ward for his support, to G. R. Odette (University of California, Santa Barbara) for helpful discussions and for providing the γ -TiAl composites, and to Eric Rosenberg for experimental assistance.

REFERENCES

1. Liu, C. T., Stiegler, J. O. and Froes, F. H., *Metals Handbook*, 1991, **2**, 913.
2. Fleischer, R. L., Dimiduk, D. M. and Lipsitt, H. A., *A. Rev. Mater. Sci.*, 1989, **19**, 231.
3. Kim, Y. W., *Acta metall. mater.*, 1992, **40**, 1121.
4. Kim, Y. W. and Dimiduk, D. M., *J. Metals*, 1991, **43**(8), 40.
5. Chan, K. S. and Kim, Y. W., *Metall. Trans. A*, 1992, **23A**, 1663.
6. Chan, K. S., *J. Metals*, 1992, **44**(5), 30.
7. Dève, H. E., Evans, A. G. and Shih, D. S., *Acta metall. mater.*, 1992, **40**, 1259.
8. Elliott, C. K., Odette, G. R., Lucas, G. E. and Shekherd, J. W., in *High-Temperature/High-Performance Composites, MRS Symp. Proc.*, Vol. 120, ed. F. D. Lemkey, A. G. Evans, S. G. Fishman and J. R. Strife. Materials Research Society, Pittsburgh, Pennsylvania, 1988, p. 95.
9. Dève, H. E., Evans, A. G., Odette, G. R., Mehrabian, R., Emiliani, M. L. and Hecht, R. J., *Acta metall. mater.*, 1990, **38**, 1491.
10. Odette, G. R., Dève, H. E., Elliott, C. K., Harigowa, A. and Lucas, G. E., in *Interfaces in Ceramic Metal Interfaces*, ed. R. Y. Lin, R. J. Arsenault, G. P. Martins and S. G. Fishman. TMS-AIME, Warrendale, Pennsylvania, 1990, p. 443.
11. Odette, G. R., Chao, B. L., Shekherd, J. W. and Lucas, G. E., *Acta metall. mater.*, 1992, **40**, 2381.
12. Venkateswara Rao, K. T., Odette, G. R. and Ritchie, R. O., *Acta metall. mater.*, 1992, **40**, 353.
13. Venkateswara Rao, K. T., Odette, G. R. and Ritchie, R. O., *Acta metall. mater.*, 1994, **42**, 893.
14. Perkins, R. A. and Meier, G. H., *J. Metals*, 1990, **17**(8), 17.
15. Soboyejo, W. O., Venkateswara Rao, K. T., Sastry, S. M. L. and Ritchie, R. O., *Metall. Trans. A*, 1993, **24A**, 585.
16. Anon, *American Society for Testing and Materials Standard E399-90*, Vol. 3.01, 1992, p. 506.
17. Anon, *American Society for Testing and Materials Standard E647-91*, Vol. 3.01, 1992, p. 674.
18. Lipsitt, H. A., Shechtman, D. and Schafrik, R. A., *Metall. Trans. A*, 1975, **6A**, 1991.
19. Venkateswara Rao, K. T., Kim, Y.-W. and Ritchie, R. O., *Scripta metall. mater.*, 1995, **33**, 459.
20. McKelvey, A. L., Venkateswara Rao, K. T. and Ritchie, R. O., *Scripta metall. mater.*, 1997, **37**, 1797.
21. Balsone, S. J., Larsen, J. M., Maxwell, D. C. and Jones, J. W., *Mater. Sci. Engng*, 1995, **A192/193**, 457.
22. Ashby, M. F., Blunt, F. J. and Bannister, M., *Acta metall.*, 1989, **37**, 1847.
23. Budiansky, B., Amazigo and Evans, A. G., *J. Mech. Phys. Solids*, 1988, **36**, 167.

24. Ritchie, R. O., Yu, W. and Bucci, R. J., *Engng Fract. Mech.*, 1989, **32**, 361.
25. Ritchie, R. O. and Dauskardt, R. H., *J. Ceram. Soc. Japan*, 1991, **99**, 1047.
26. Dauskardt, R. H. and Ritchie, R. O., *Closed Loop*, 1989, **27**, 7.
27. Dauskardt, R. H., *Acta metall. mater.*, 1993, **41**, 2765.
28. Laird, C. and Smith, G. C., *Phil. Mag.*, 1963, **8**, 1945.
29. Pelloux, R. M., *Trans. Am. Soc. Metals*, 1969, **62**, 281.
30. Jata, K. V., Gerberich, W. W. and Beevers, C. J., in *Fatigue at Low Temperatures*, ASTM STP 857, ed. R. I. Stephens. ASTM, Philadelphia, Pennsylvania, 1985, p. 102.
31. Moody, N. R. and Gerberich, W. W., *Mater. Sci. Engng*, 1979, **41**, 271.